Journal of Physics Research and Education, Volume 3, March 2026

Flexible PVDF-Based Portable Self-Powered Piezoelectric Nanogenerator for Sustainable Energy Harvesting

Prosenjit Biswas*

Physics Department, Kalimpong College, Kalimpong- 734301, India

In this study, biocompatible poly(vinylidene fluoride) (PVDF) films were successfully synthesized through an in situ fabrication process, which enables uniform structural formation and enhanced piezoelectric properties. The prepared PVDF films exhibited excellent functional characteristics, including a significant piezoelectric coefficient ($d_{33} \approx 33.8$ pC N^{-1}) along with a remarkably high dielectric constant ($\sim 20 \times 10^5$) at a low operating frequency of 20 Hz. Based on these optimized PVDF films, we further designed and developed a biocompatible, highly durable, and cost-effective piezoelectric nanogenerator, referred to as PENG. The fabricated device demonstrates outstanding electrical output performance when subjected to simple mechanical stimuli such as a gentle finger touch. Specifically, the nanogenerator produces an open-circuit voltage of approximately 52 V and a short-circuit current of about 1.9 μA, resulting in a power density of nearly 56 mW cm^{-3}. These results highlight the superior energy harvesting capability of the device even under low mechanical force conditions.

I. INTRODUCTION

At the current stage of global energy transition, the progressive depletion of fossil fuel resources has intensified the search for sustainable, renewable and environmentally friendly energy sources. The extensive consumption of conventional fossil fuels such as petroleum and coal has resulted in severe environmental challenges, including air and water pollution, greenhouse gas emissions and climate change. Consequently, the exploration of alternative energy resources such as solar, wind, rain, and geothermal energy has emerged as one of the most significant research areas in modern energy science. These renewable sources are considered promising solutions for addressing the growing global energy demand while simultaneously reducing environmental degradation. In recent decades, the rapid advancement of modern electronic technologies has led to the widespread use of multifunctional electronic devices such as smartphones, tablets, laptops, wearable electronics, and various types of sensors in everyday life. These devices typically rely on conventional electrochemical energy storage systems, particularly lithium-ion batteries, which provide long-duration operation but present several limitations including finite lifetime, environmental concerns, and challenges related to disposal and recycling [1–7]. As a result, there has been increasing interest in developing self-powered systems that can harvest energy from ambient sources to reduce dependence on traditional batteries.

To address this challenge, the scientific community has devoted considerable effort toward developing green energy harvesting technologies capable of converting abundant energy resources

* prosenbiswas1993@gmail.com

present in nature—such as solar radiation, ocean waves, and wind energy—into usable electrical power. In addition to natural sources, mechanical energy generated from human activities, including walking, body motion, and even speaking, has also been explored as a viable energy resource. Researchers have further attempted to integrate energy harvesting devices with energy storage systems to create hybrid systems capable of simultaneously generating and storing electrical energy. Such integrated systems are considered promising for addressing both global energy demands and environmental concerns in the electronics industry [5, 8–14]. Recently, several studies have focused on the design of multifunctional devices that combine energy harvesting and electrical energy storage components within a single integrated unit [5, 14]. Although numerous materials and device architectures have been explored for this purpose, achieving high efficiency and practical applicability remains a significant challenge in meeting the demands of modern society [6, 15–18]. Among the various energy harvesting technologies, piezoelectric nanogenerators (PENGs) have emerged as highly promising devices capable of converting mechanical energy directly into electrical energy through the piezoelectric effect [1, 19, 20]. Since their initial development, prototype PENGs have been fabricated using a variety of piezoelectric materials such as lead zirconate titanate (PZT), $ZnSnO_3$, ZnO, $BaTiO_3$, (Na,K)NbO_3, and other perovskite-based materials. Although these materials exhibit high piezoelectric performance, their practical application is often limited due to issues such as high density, mechanical rigidity, limited flexibility, and potential toxicity, which restrict their use in flexible and wearable electronic devices [21–28].

To overcome these limitations, electroactive polymers, particularly poly(vinylidene fluoride) (PVDF) and its copolymers, have attracted considerable attention as alternative piezoelectric materials. PVDF offers several advantages, including lightweight nature, mechanical flexibility, chemical stability, cost-effectiveness, and excellent biocompatibility, making it highly suitable for the fabrication of flexible piezoelectric nanogenerators [5, 6, 20, 29–31]. PVDF is a thermoplastic semi-crystalline polymer that can crystallize into five distinct phases, namely α, β, γ, δ, and ϵ, depending on the chain conformation and orientation of the $–CF_2$ and $–CH_2$ dipoles. Among these phases, α, β, and γ phases are the most commonly observed crystalline structures. The α-phase, characterized by a TGTG′ (trans–gauche–trans–gauche) conformation, is the most thermodynamically stable and is typically formed during conventional melt crystallization. The γ-phase, having a TTGTTG′ conformation, exhibits moderate piezoelectric properties. In contrast, the β-phase, which possesses an all-trans (TTTT) planar zigzag configuration, is highly polar in nature and exhibits the highest piezoelectric, ferroelectric, and pyroelectric properties, along with excellent dielectric characteristics and mechanical strength [5, 20, 32–36].

Therefore, the development of simple, cost-effective methods for inducing the electroactive β-phase in PVDF is a key requirement for its application in various electronic and energy-related technologies, including nanogenerators, actuators, sensors, biomedical devices, and energy storage systems. Traditionally, β-phase formation in PVDF has been achieved through techniques such as electrical poling under high electric fields and mechanical stretching of polymer films. Additionally, electrospinning techniques have also been widely employed to promote the formation of β-phase crystalline structures in PVDF nanofibers [37–39].

However, in recent years, researchers have demonstrated that self-poled β-phase nucleation can be achieved without mechanical stretching by incorporating different types of functional fillers into the PVDF matrix. These fillers include metal oxide nanoparticles, metallic nanoparticles, ceramic nanoparticles, carbon nanotubes, metal salts, organic molecules, clays and graphene-based materials [6, 8, 14, 40–53]. The incorporation of such fillers not only facilitates β-phase nucleation but also significantly enhances the dielectric properties of PVDF due to increased interfacial po-

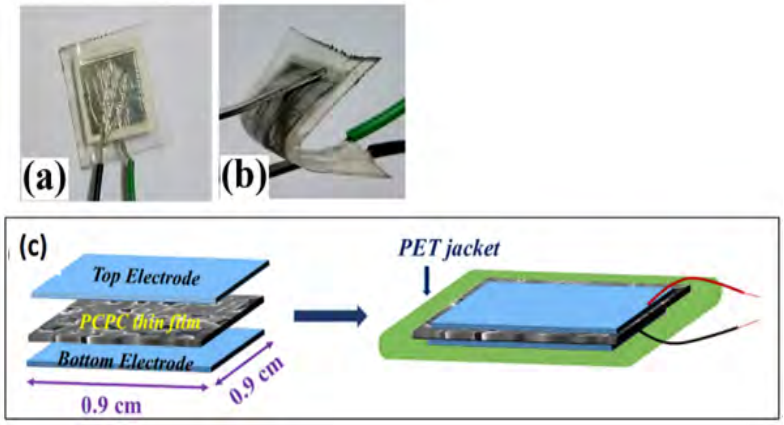

FIG. 1. (a) and (b) Snapshot and digital photograph of the flexibility check of the PENG. (c) Fabrication process of the PENG is schematically illustrated.

larization and dipole alignment within the composite structure. The simultaneous enhancement of electroactive β-phase crystallinity and dielectric properties in PVDF-based materials offers great potential for developing high-performance mechanical energy harvesting devices based on the piezoelectric effect. Moreover, these materials also exhibit the capability to store electrical energy, enabling the development of multifunctional devices that combine energy harvesting and energy storage functionalities [5, 8, 14, 20].

II. EXPERIMENT

III. RESULTS AND DISCUSSIONS

Materials : In our present work the materials taken are poly(vinylidene fluoride) (Mw: 250 000 GPC, Mn: 71 000, Sigma-Aldrich, Germany.), dimethyl sulfoxide (DMSO) (Merck, India), aluminium foil (Sigma-Aldrich, Germany), FTO coated glass (Sigma-Aldrich, Germany).

Synthesis of PVDF based thin films : Initially, a 5 mass % clear solution of PVDF in DMSO has been prepared by dissolving 250 mg PVDF into 5 ml DMSO with the help of magnetic stirrer at 60°C. Then the films of PVDF have been obtained by casing the mixture in clean Petri dishes and dried at 80°C for complete evaporation of DMSO in a dust free oven. At the same time same concentration of pure PVDF thin film has been prepared under the same condition.

Fabrication of prototype PENG : For the fabrication of the piezoelectric nanogenerator, aluminum (Al) electrodes were carefully attached to both sides of the highly electroactive PCPC thin film, which had approximate dimensions of 0.9 cm $\times$ 0.9 cm with a thickness of about 22 μm. Subsequently, two copper wires were connected to the respective electrodes to facilitate the measurement of the electrical output performance of the prototype PENG. Finally, the entire device was encapsulated using a poly(ethylene terephthalate) (PET) jacket to provide mechanical stability and environmental protection. The digital photograph of the fabricated PENG device and the schematic illustration of the fabrication process are presented in Fig. 1(a), (b) and Fig. 1(c).

Characterization technique and measurement methods : The phase transformation and crystalline structure of the PVDF films were characterized using X-ray diffraction (XRD) analysis. The measurements were carried out with an X-ray diffractometer (Model D8, Bruker AXS Inc., Madison, WI) employing Cu–Kα radiation. The diffraction patterns were recorded over a 2θ range of 15°–40° at room temperature. The instrument was operated at an accelerating voltage of 35 kV and a current of 35 mA, with a scan speed of 0.3 s per step. Furthermore, the nucleation and presence of the electroactive β-phase in the PVDF samples were confirmed using Fourier Transform Infrared Spectroscopy (FTIR) (Model FTIR-8400S, Shimadzu). Based on the obtained IR spectra, the fraction of β-phase (F(β)) present in pure PVDF and the composite samples was quantitatively estimated using the Lambert–Beer equation, given as [5, 8],

$$F(\beta) = \frac{A_\beta}{\left(\frac{K_\beta}{K_\alpha}\right) A_\alpha + A_\beta}, \tag{1}$$

where K_α (6.1×10^4 cm^2 mol^{-1}) and K_β (7.7×10^4 cm^2 mol^{-1}) are the absorption coefficients and A_α, A_β are the absorbance intensities at 764 cm^{-1} and 840 cm^{-1} respectively. The output performance of the CPNG device was investigated using a digital storage oscilloscope (Keysight, DSO-X 3012A). In addition, the electrical output characteristics of LCPP were measured using a high-precision electrometer (Keysight B2985A) and a digital multimeter (Agilent U1252A) to ensure accurate electrical characterization.

In this study, we focus on the optimization and successful characterization of electroactive β-phase nucleation and enhanced dielectric properties in PVDF composite thin films. Furthermore, based on these optimized materials, we aim to design and develop a biocompatible, low-cost, and flexible piezoelectric nanogenerator (PENG) capable of efficiently converting mechanical energy into electrical energy through the piezoelectric effect.

A. Characterization of CP-Incorporated PVDF thin films

X-ray diffraction spectra analysis : Figure 2(a) denotes the result of nucleation of the electroactive β-phase of PVDF by using X-ray diffraction pattern analysis. Here, the peaks at $2\theta = 17.5°$, $18.3°$, $19.9°$, $26.4°$ and $38.5°$ represent the nonpolar α- crystals of pure PVDF. In the diffraction spectra of the films, a characteristic peak prominently appears at $2\theta = 20.6°$, which indicates the formation of electroactive β-phase along with the vanishing of all characteristic peaks of α phase [5, 32].

Fourier Transform infrared spectroscopy evaluation : The authentication of the electroactive β-polymorph formation have been established by analyzing the FTIR spectrum represented in Fig. 2(c). The characteristics absorbance bands appears at 488 cm^{-1} (CF_2 bonds waging), 532 cm^{-1} (bending of CF_2 bonds), 615 and 764 cm^{-1} (CF_2 skeletal bending), 796 and 975 cm^{-1} (CH_2 rocking) which indicate the existence of nonpolar α-phase of unblended PVDF along with a very small intense absorbance band at 840 cm^{-1} (CH_2 rocking, CF_2 stretching and skeletal C-C stretching) which is due to the β-crystallite [14, 32].

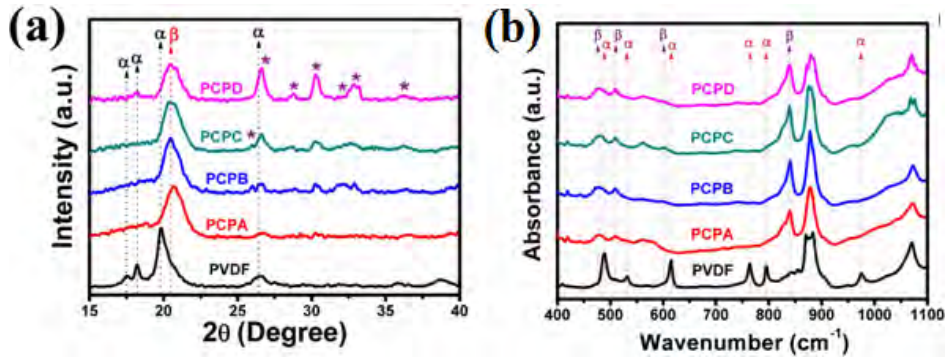

FIG. 2. (a) XRD spectra of PVDF thin films for different volume concentrations. (b) FTIR pattern of PVDF thin films.

B. Output Performance of PENG

The output performance of the CPNG, including the open-circuit voltage (Voc), short-circuit current (Isc), and the resulting power density, was generated under periodic axial pressure applied by human finger tapping. The corresponding electrical output characteristics are presented in Figs. 3(a), 3(b) and 3(c), respectively. The output performance, including the open-circuit voltage and power density of our desired CPNG under a periodic constant force of about 14 N at different frequencies, has been investigated, as shown in Fig. 3(d). The maximum output performance of the PENG was obtained at an operating frequency of approximately 6 Hz. At this frequency, the device generated an open-circuit voltage of about 52 V and a short-circuit current of approximately 1.9 μA, corresponding to a maximum power density of nearly 56 mW cm^{-3} under periodic finger-induced mechanical stimulation, as illustrated in Fig. 3(e). At higher frequencies, the output performance gradually decreased. This reduction may be attributed to impedance mismatch in the measurement system, which limits the ability of the PENG to fully restore its original mechanical state during rapid excitation cycles. In contrast, at 6 Hz the device exhibits an impedance matching with the external measurement circuit, resulting in the optimized electrical output performance.

IV. CONCLUSIONS

In the present work, we have successfully fabricated a prototype piezoelectric nanogenerator (PENG) that demonstrates an efficient capability to directly convert mechanical energy into electrical energy through the piezoelectric effect. Under periodic mechanical stimulation, such as gentle finger tapping, the fabricated PENG generates a significant open-circuit voltage of about 52 V along with a short-circuit current of nearly 1.9 μA. These electrical outputs clearly demonstrate the high performance of the device and confirm its suitability as a self-powered energy harvesting system. Moreover, the generated electrical energy from the device is sufficient to directly illuminate multiple light-emitting diodes (LEDs), which highlights its practical capability for powering small electronic components without relying on conventional batteries. This result demonstrates the promising potential of the fabricated PENG for sustainable and portable power generation, especially for low-power electronic devices. Looking ahead, the developed device has strong potential for practical real-world applications. In future work, we aim to further optimize the

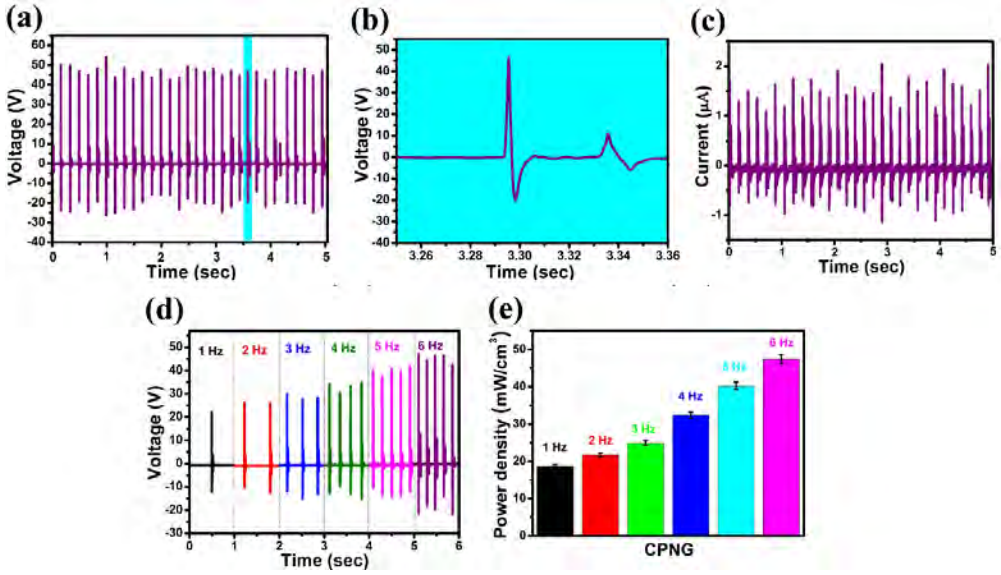

FIG. 3. (a)–(c) Open-circuit voltage generated by the PENG, the magnified view of the output voltage signal, and the corresponding short-circuit current produced under periodic finger tapping. (d)–(e) Frequency-dependent variation of output voltage and power density under a constant applied force.

performance of this nanogenerator so that it can be utilized to operate small electronic devices such as digital clocks, toys, and portable sensors, as well as charge mobile phones and other small portable electronic gadgets. Such developments could contribute significantly to the advancement of self-powered electronic systems, reducing dependence on traditional energy storage devices and promoting the development of environmentally friendly and sustainable energy technologies.

Acknowledgment : I am thankful to University Grants Commission (UGC), Government of India and Anusandhan National Research Foundation for financial support.

[1] J. H. Lee *et al.*, J. Mater. Chem. A **4**, 7983 (2016).
[2] A. Waseem *et al.*, Nano Energy **60**, 413 (2019).
[3] Y. Qin, X. Wang, and Z. L. Wang, Nature **451**, 809 (2008).
[4] M. Grätzel, Nature **414**, 338 (2001).
[5] P. Thakur *et al.*, Nano Energy **44**, 456 (2018).
[6] P. Biswas *et al.*, ACS Sustainable Chem. Eng. **7**(5), 4801 (2019).
[7] L. Xing *et al.*, Nano Energy **10**, 44 (2014).
[8] F. Khatun *et al.*, Energy Convers. Manage. **171**, 1083 (2018).
[9] W. Yang *et al.*, ACS Nano **7**, 11317 (2013).
[10] J. Liu *et al.*, Nanoscale **8**, 4938 (2016).
[11] L. Gu *et al.*, Nano Lett. **13**, 91 (2012).
[12] C. Zhao *et al.*, Nano Energy **57**, 440 (2019).
[13] X. Wang *et al.*, Science **316**, 102 (2007).

[14] S. Roy *et al.*, ACS Appl. Mater. Interfaces **9**, 24198 (2017).
[15] A. Ramadoss *et al.*, ACS Nano **9**, 4337 (2015).
[16] Q. Zhang *et al.*, Adv. Mater. **21**, 4087 (2009).
[17] X. Xue *et al.*, Nano Lett. **12**, 5048 (2012).
[18] H. He *et al.*, Sci. Bull. **64**, 1409 (2019).
[19] K. I. Park *et al.*, Adv. Mater. **26**, 2514 (2014).
[20] N. A. Hoque *et al.*, ACS Appl. Mater. Interfaces **9**, 23048 (2017).
[21] H. B. Kang *et al.*, ACS Appl. Mater. Interfaces **6**, 10576 (2014).
[22] S. Xu *et al.*, Nano Lett. **13**, 2393 (2013).
[23] Z. H. Lin *et al.*, J. Phys. Chem. Lett. **3**, 3599 (2012).
[24] S. H. Zhang *et al.*, J. Mater. Chem. C **7**, 4760 (2019).
[25] J. M. Wu *et al.*, RSC Adv. **3**, 25184 (2013).
[26] N. A. Hoque *et al.*, J. Mater. Chem. A **6**, 13848 (2018).
[27] A. Sultana *et al.*, ACS Appl. Mater. Interfaces **10**, 4121 (2018).
[28] R. Ding *et al.*, Nano Energy **37**, 126 (2017).
[29] C. Chang *et al.*, Nano Lett. **10**, 726 (2010).
[30] H. He *et al.*, Nano Energy **39**, 590 (2017).
[31] X. Xue *et al.*, Adv. Energy Mater. **4**, 1301329 (2014).
[32] P. Martins *et al.*, Prog. Polym. Sci. **39**, 683 (2014).
[33] P. Thakur *et al.*, RSC Adv. **5**, 28487 (2015).
[34] N. A. Hoque *et al.*, RSC Adv. **6**, 29931 (2016).
[35] P. Thakur *et al.*, Phys. Chem. Chem. Phys. **17**, 13082 (2015).
[36] Y. Zhang *et al.*, ACS Appl. Mater. Interfaces **4**, 65 (2012).
[37] L. He and S. C. Tjong, RSC Adv. **3**, 22981 (2013).
[38] S. Bao *et al.*, Carbon **49**, 1758 (2011).
[39] J. Andrew and D. Clarke, Langmuir **24**, 670 (2008).
[40] Y. J. Li *et al.*, Appl. Phys. Lett. **89**, 072902 (2006).
[41] S. F. Mendes *et al.*, J. Mater. Sci. **47**, 1378 (2012).
[42] W. Wu *et al.*, J. Phys. Chem. C **116**, 24887 (2012).
[43] P. Thakur *et al.*, RSC Adv. **6**, 26288 (2016).
[44] P. Thakur *et al.*, Phys. Chem. Chem. Phys. **17**, 1368 (2015).
[45] D. Mandal *et al.*, Mater. Lett. **73**, 123 (2012).
[46] M. Benz *et al.*, Macromolecules **35**, 2682 (2002).
[47] J. K. Yuan *et al.*, J. Phys. Chem. C **115**, 5515 (2011).
[48] S. Roy *et al.*, RSC Adv. **6**, 21881 (2016).
[49] P. Wang *et al.*, Langmuir **28**, 4776 (2012).
[50] E. Thomas *et al.*, Polymer **115**, 70 (2017).
[51] G. Peng *et al.*, J. Elastomers Plast. **48**, 251 (2016).
[52] P. Thakur *et al.*, Appl. Clay Sci. **99**, 149 (2014).
[53] K. Pal *et al.*, Langmuir **26**, 3609 (2009).